



ALK-Fusion Transcripts Can Be Detected in Extracellular Vesicles (EVs) from Nonsmall Cell Lung Cancer Cell Lines and Patient Plasma: Toward EV-Based Noninvasive Testing

Estela Sánchez-Herrero,^{a,b,†} Carmen Campos-Silva,^{c,†} Yaiza Cáceres-Martell,^c Lucía Robado de Lope,^a Sandra Sanz-Moreno,^a Roberto Serna-Blasco,^a Alejandro Rodríguez-Festa,^a Dunixe Ares Trotta,^a Paloma Martín-Acosta,^d Cristina Patiño,^e María José Coronado,^f Alexandra Beneitez,^g Ricardo Jara,^g Nerea Lago-Baameiro,^h Tamara Camino,^h Alberto Cruz-Bermúdez,^a María Pardo,^h Víctor González-Rumayor,^b Mar Valés-Gómez ,^{c,*} Mariano Provencio,^{a,i} and Atocha Romero ^{a,i,*}

BACKGROUND: *ALK* rearrangements are present in 5% of nonsmall cell lung cancer (NSCLC) tumors and identify patients who can benefit from *ALK* inhibitors. *ALK* fusions testing using liquid biopsies, although challenging, can expand the therapeutic options for *ALK*-positive NSCLC patients considerably. RNA inside extracellular vesicles (EVs) is protected from RNases and other environmental factors, constituting a promising source for noninvasive fusion transcript detection.

METHODS: EVs from H3122 and H2228 cell lines, harboring *EML4-ALK* variant 1 (E13; A20) and variant 3 (E6a/b; A20), respectively, were successfully isolated by sequential centrifugation of cell culture supernatants. EVs were also isolated from plasma samples of 16 *ALK*-positive NSCLC patients collected before treatment initiation.

RESULTS: Purified EVs from cell cultures were characterized by transmission electron microscopy (TEM), nanoparticle tracking analysis (NTA), and flow cytometry. Western blot and confocal microscopy confirmed the expression of EV-specific markers as well as the expression of *EML4-ALK*-fusion proteins in EV fractions from H3122 and H2228 cell lines. In addition, RNA from EV fractions derived from cell culture was analyzed by digital PCR (dPCR) and *ALK*-fusion transcripts were clearly detected. Similarly, plasma-derived EVs were

characterized by NTA, flow cytometry, and the ExoView platform, the last showing that EV-specific markers captured EV populations containing *ALK*-fusion protein. Finally, *ALK* fusions were identified in 50% (8/16) of plasma EV-enriched fractions by dPCR, confirming the presence of fusion transcripts in EV fractions.

CONCLUSIONS: *ALK*-fusion transcripts can be detected in EV-enriched fractions. These results set the stage for the development of EV-based noninvasive *ALK* testing.

Introduction

Genomic rearrangements involving the oncogenic anaplastic lymphoma kinase (*ALK*) gene occur in 3 to 5% of nonsmall cell lung cancer (NSCLC) tumors (1, 2). So far, nearly 30 different *ALK*-fusion partners have been described, with *EML4* being the most common (3, 4). A wide therapeutic arsenal is currently available to tackle *ALK*-positive NSCLC tumors (5–7). Testing for *ALK* fusions is thus mandatory since the identification of *ALK* rearrangements significantly expands the therapeutic opportunities and life expectancy of these patients. However, the availability of tumor biopsies is sometimes limited for NSCLC patients, mostly due to the anatomical location of the tumor and the advanced age of these patients. Biomarker testing using liquid biopsies can

^aLiquid Biopsy Laboratory, Medical Oncology Department, Instituto de Investigación Sanitaria Puerta de Hierro-Segovia de Arana, Majadahonda, Spain; ^bI+D Department, Atrys Health, Barcelona, Spain; ^cDepartment of Immunology and Oncology, Spanish National Centre for Biotechnology, CNB-CSIC, Madrid, Spain; ^dPathology Department, Instituto de Investigación Sanitaria Puerta de Hierro-Segovia de Arana, Majadahonda, Spain; ^eElectron Microscopy Unit Centro Nacional de Biotecnología, CSIC, Madrid, Spain; ^fConfocal Microscopy Core Facility, Instituto de Investigación Sanitaria Puerta de Hierro-Segovia de Arana, Majadahonda, Spain; ^gImmunostep, S.L., Salamanca, Spain; ^hGrupo Obesidómica, Área de Endocrinología, Instituto de Investigación Sanitaria de Santiago (IDS), Hospital Clínico Universitario de Santiago, Santiago de Compostela, Spain;

ⁱMedical Oncology Department, Hospital Universitario Puerta de Hierro-Majadahonda, Majadahonda, Spain.

*Address correspondence to: A.R. at Medical Oncology Department, Hospital Puerta de Hierro, Calle Joaquín Rodrigo, 1, 28222 Majadahonda, Madrid, Spain. Fax 911917872; e-mail atocha10@hotmail.com. M.V.-G. at Immunology and Oncology Department, Spanish National Centre for Biotechnology, CNB-CSIC, Calle Darwin, 3, 28049 Madrid, Spain. Fax 915854506; e-mail mvales@cnb.csic.es.

[†]These authors contributed equally to this work.

Received October 22, 2021; accepted January 12, 2022.

<https://doi.org/10.1093/clinchem/hvac021>

potentially overcome these limitations. Indeed, genomic profiling of liquid biopsies is integrated in NSCLC guidelines (8). Still, the identification of genomic rearrangements using liquid biopsies remains challenging. The identification of *ALK* translocation in circulating tumor DNA (ctDNA) is complicated as the rearrangement involves a large number of bases, breakpoints are usually unknown, and ctDNA is highly fragmented. Indeed, a sensitivity of 40% has been reported for next-generation sequencing assays in detecting oncogenic fusions in plasma cell-free DNA (9). Likewise, circulating free RNA (cfRNA) is rapidly degraded by RNases present in the bloodstream. However, RNAs carried in extracellular vesicles (EVs) are a priori protected from RNases. The use of EVs for noninvasive biomarker testing has several advantages. First, EVs are stable and they protect RNAs from degradation in the extracellular environment (10); second, nearly all types of cells can release EVs (11); and third, EV isolation methods from plasma samples can be automated so that the process can be scaled for high-throughput applications and therefore be adapted to the clinics.

In this preclinical study, we aimed to elucidate whether *ALK* fusions were detectable in EVs derived from NSCLC. To this aim, H3122 and H2228 NSCLC cell lines were used and EV enrichment protocols were followed to examine the presence of translocation messenger and protein products. The protocol was then optimized for the analysis of plasma samples from 16 *ALK*-positive NSCLC patients.

Materials and Methods

PLASMA SAMPLES

Plasma samples from 16 *ALK*-positive NSCLC patients were collected before treatment initiation at Hospital Puerta de Hierro-Majadahonda. The study protocol was approved by the Hospital Puerta de Hierro Ethics Committee (internal code 79-18). Appropriate written informed consent was obtained from all patients prior to enrollment in the study. Briefly, eligibility criteria included patients who were 18+ years of age and with a pathologically confirmed diagnosis of stage IV NSCLC with an *ALK* translocation.

EVS ISOLATION

Cell lines from NSCLC (H3122 and H2228) harboring an *ALK* translocation were grown. Conditions regarding tissue culture are available in the Methods in the online Data Supplement. As a control, the metastatic melanoma cell line (Ma-Mel-55) was used (12). Detailed information about EV isolation is available in the online [Supplemental Methods](#). Briefly, cell culture supernatants (200 mL) were centrifuged twice for 10 min at

200g, followed by 2 centrifugations at 500g for 10 min and 1 centrifugation of 30 min at 10 000g. Finally, ultracentrifugation at 100 000g for 2 h at 4°C with no brake was carried out to collect EVs.

Plasma samples were collected in a 10-mL Streck Cell-Free DNA BCT[®] tube. Cell debris were removed by centrifugation at 2000g for 10 min at 4°C. Plasma samples were diluted in PBS (1:3) and centrifuged once at 110 000g for 2 h at 4°C with no brake to collect EVs.

EV QUANTITATION

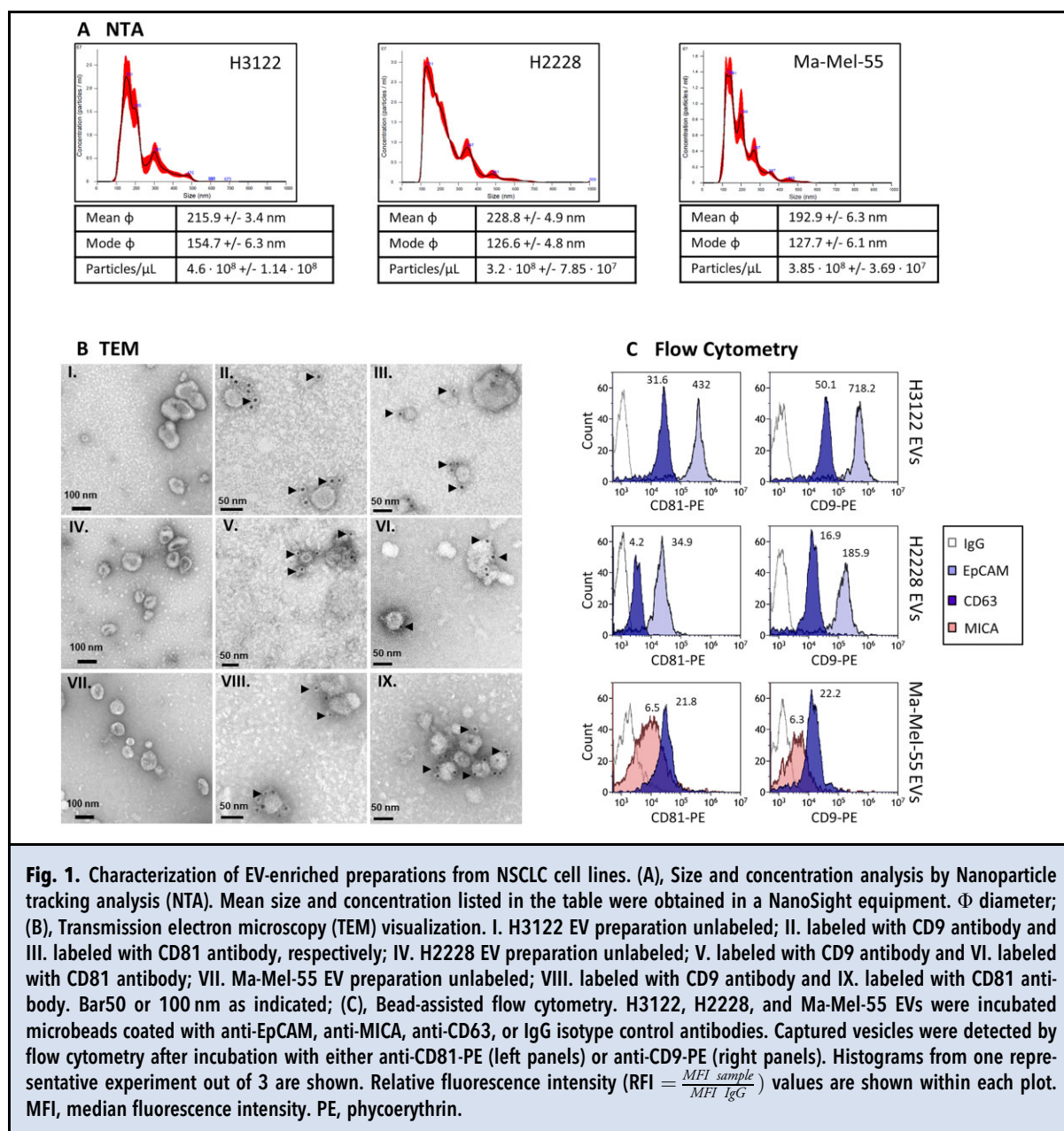
The concentration and size of particles in the EV preparations were characterized by nanoparticle tracking analysis (NTA) in a NanoSight NS500 (Malvern Instruments Ltd) equipped with a 405 nm laser. Three different captures of 60 s were analyzed per sample. The settings used were camera level 12 (EVs from cell lines), 10 (EVs from NSCLC plasma samples), focus between -15 and +15, threshold 10, and temperature 25°C.

TRANSMISSION ELECTRON MICROSCOPY (TEM) AND GOLD IMMUNOLABELING

Detailed information about TEM protocol is available in the online [Supplemental Methods](#). Briefly, H3122 and H2228 EV preparations were diluted 1:10 in HBS and adsorbed on a formvar-carbon coated grid, and either stained with 2% uranyl acetate and analyzed directly in the TEM or labeled with antibodies as follows. After blocking, grids were incubated with the primary antibody, either anti-CD9 clone VJ120 (Immunostep, S.L.) or anti-CD81 clone 5A6 (Santa Cruz Biotechnology), blocked again and incubated with goat anti-mouse fab2'-gold 10 nm (BBI International). Finally, grids were stained with uranyl acetate 2%, dried, and analyzed using a Jeol JEM 1011 (JEOL Ltd) electron microscope operating at 100 kV with a CCD camera Gatan Erlangshen ES1000W (Gatan Ink).

CONFOCAL MICROSCOPY

Detailed information about confocal microscopy protocols is available in the [Supplemental Methods](#). Briefly, a drop of EV pellet was put on a 35-mm imaging dish with a polymer coverslip bottom for high-end microscopy, dried, fixed with 4% *p*-formaldehyde and treated with NH₄Cl 50 mmol/L. After permeabilization with 0.2% Triton X-100, samples were blocked with 5% BSA, incubated with anti-CD63 antibody (Merck Millipore), and incubated with goat anti-mouse secondary antibody conjugated to ALEXA 546 or 488 (Invitrogen-Life Technologies). For a second immunodetection, samples were blocked again, incubated with anti-*ALK* antibody (Ventana D5F3; Cell Signaling Technology) or with anticalreticulin antibody (NB600-101; Novus Biologicals) and incubated with goat anti-



rabbit secondary antibody conjugated to ALEXA 488 or 546 (Invitrogen-Life Technologies).

Fluorescence in situ hybridization (FISH) was performed using fixed EV-enriched samples and parent cells. EV-enriched samples and parent cells were permeabilized with 0.2% Triton X-100, dehydrated with 50%, 70%, and 100% ethanol, and incubated with a biotinylated *EML4-ALK* RNA probe. The specimens were incubated with hybridization buffer, washed, blocked with BSA 5%, and incubated with

antistreptavidin antibody conjugated to ALEXA 546 (Invitrogen-Life Technologies). Nonpermeabilized and nondehydrated cells were incubated with a biotinylated *EML4-ALK* RNA probe, as a control condition. Nuclei were stained with TO-PRO-3 (Thermo Fisher Scientific). Images were collected with a TCS SP5 confocal microscope (Leica Microsystems) using a $\times 63$ HCX PL APO (1.25–1.52 numerical aperture) oil-immersion objective and $\times 3$ zoom. For immunofluorescence, the following excitation and emission parameters

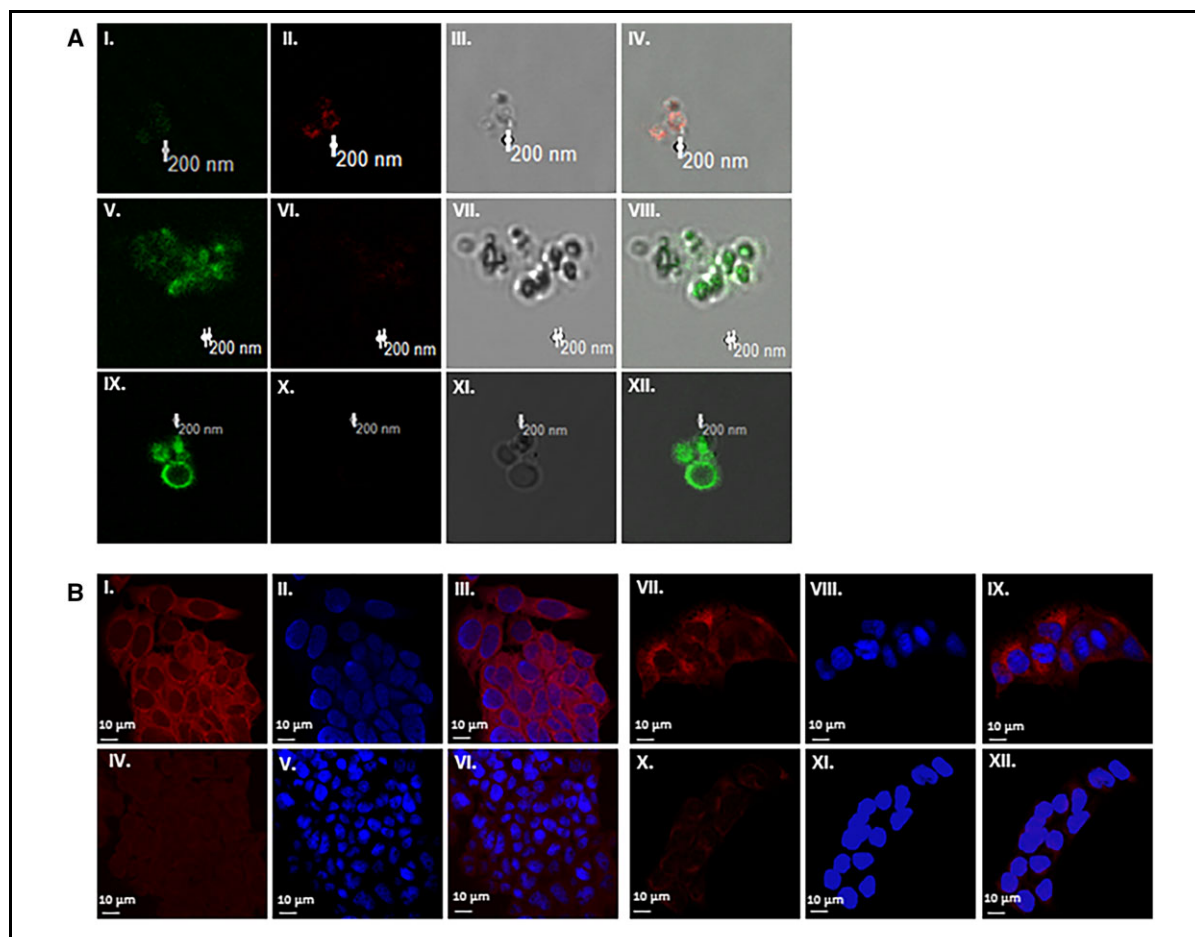


Fig. 2. Characterization of EV-enriched preparations from NSCLC cell lines by confocal microscopy visualization. (A), Double immunofluorescence in EV preparations. I. H3122 EVs stained with *EML4-ALK* antibody (green); II. H3122 EVs stained with CD63 antibody (red); III. H3122 EVs in bright field; IV. Merge; V. Ma-Mel-55 EVs stained with CD63 antibody (green); VI. Ma-Mel-55 EVs stained with *EML4-ALK* antibody (red); VII. Ma-Mel-55 EVs in bright field; VIII. Merge; IX. H3122 EVs stained with calreticulin antibody (green); X. H3122 EVs stained with calreticulin antibody (red); XI. H3122 EVs in bright field; XII. Merge; (B), FISH RNA with biotinylated RNA assay for *EML4-ALK* variant 1 in H3122 cells, I. H3122 permeabilized cells labeled with *EML4-ALK* variant 1 biotinylated RNA assay (red); II. H3122 permeabilized cells labeled with TO-PRO-3 (blue); III. Merge; IV. H3122 nonpermeabilized cells labeled with *EML4-ALK* variant 1 biotinylated RNA assay (red); V. H3122 nonpermeabilized cells labeled with DAPI (blue); VI. Merge; VII. H2228 permeabilized cells labeled with *EML4-ALK* variant 3 biotinylated RNA assay (red); VIII. H2228 permeabilized cells labeled with DAPI (blue); IX. Merge; X. H2228 nonpermeabilized cells labeled with *EML4-ALK* variant 3 biotinylated RNA assay (red); XI. H2228 nonpermeabilized cells labeled with DAPI (blue); XII. Merge; (C), FISH RNA with biotinylated RNA assay for *EML4-ALK* variants in EV preparations, I. H2228 EVs with *EML4-ALK* variant 3 biotinylated RNA assay (red); II. H2228 EVs in bright field; III. H2228 Merge EV preparation; IV. Ma-Mel-55 EVs with *EML4-ALK* variant 3 biotinylated RNA assay (red); V. Ma-Mel-55 EVs in bright field; VI. Merge Ma-Mel-55 EV preparation; VII. H3122 EVs with *EML4-ALK* variant 1 biotinylated RNA assay (red); VIII. H3122 EVs in bright field; IX. H3122 Merge EV preparation; X. Ma-Mel-55 EVs with *EML4-ALK* variant 1 biotinylated RNA assay (red); XI. Ma-Mel-55 EVs in bright field; XII. Merge Ma-Mel-55 EV preparation. Bars represent 200 nm.

were used (546 nm, 557–572 nm) for CD63 and *EML4-ALK* signal, (488 nm, 500–540 nm) for *EML4-ALK* and calreticulin signal, and (633 nm, 645–750 nm) for TO-PRO-3 signal. Two different lasers were used independently for each fluorophore (ALEXA 488, ALEXA 546).

FLOW CYTOMETRY

Here 2 μL of purified EVs from H3122 (1×10^8 particles) and H2228 (1×10^9 particles) cell lines and 3 NSCLC plasma samples ($1.7\text{--}3.2 \times 10^8$ particles) were incubated overnight at room temperature with 3000 microbeads coated with anti-CD63 (Clone TEA3/18),

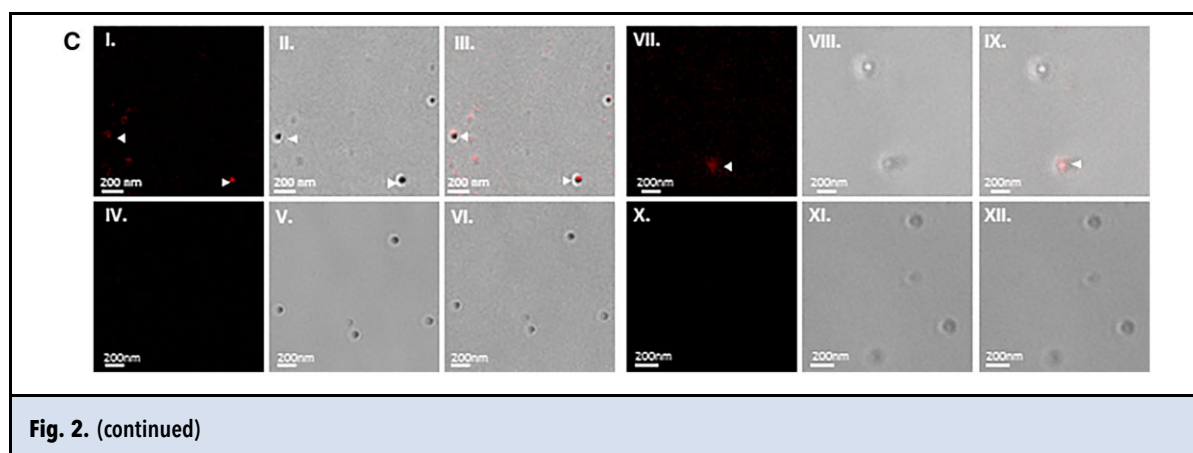


Fig. 2. (continued)

anti-EpCAM (Clone VU-1D9) or Isotype (IgG1; MOPC21) (Immunostep, S.L.) in a final volume of 25 μ L of PBS containing 1% casein (Biorad, 1 \times PBS blocker). Subsequently, beads were stained with either anti-CD9 (VJ1/20) or anti-CD81 (M-38), PE-conjugated antibodies (Immunostep, S.L.) for 1 h at 4 $^{\circ}$ C. Data were acquired using CytoFLEX flow cytometer and analyzed using Kaluza software (both Beckman Coulter), as previously described (13).

DOT BLOT

Here, 3×10^8 particles from each EV preparation were treated with HBS 1% SDS or with HBS only, adsorbed onto a nitrocellulose membrane, dried, and blocked with PBS-T (PBS 0.1% Tween-20) containing 5% non-fat dry milk for 1 h, followed by a 1 h incubation with primary antibodies at 4 $^{\circ}$ C; mouse anti-*EML4-ALK* variants [5A4 at 2.6 μ g/mL (Leica Biosystems)] and anti-CD9 at 1 μ g/mL (clone VJ120, Immunostep, S.L.). The membranes were then incubated for 1 h at RT with 0.4 μ g/mL Alexa-700-conjugated goat anti-mouse secondary antibody (ThermoFisher). Proteins were visualized using the Odyssey Infrared system (LI-COR Biosciences).

CELL LYSATES AND WESTERN BLOT

Detailed information about cell lysates and western blot is available in the [Supplemental Methods](#). Briefly, Cell lysates were prepared with 1% NP40 TNE buffer containing protease inhibitors. 50 μ g of total lysate proteins and 50 μ L of the EV-enriched preparation were run in 12% SDS-PAGE. Proteins were transferred to nitrocellulose membranes with Trans-Blot[®] Turbo[™] Transfer Packs (BioRad). Membranes were blocked and incubated with primary antibodies for *EML4-ALK* variants [5A4 antibody (Leica Biosystems)], CD63, CD81 and CD9 tetraspanins [MEM259; MEM-38; and MEM62, respectively (a kind gift from Vaclav Horejsi, Czech

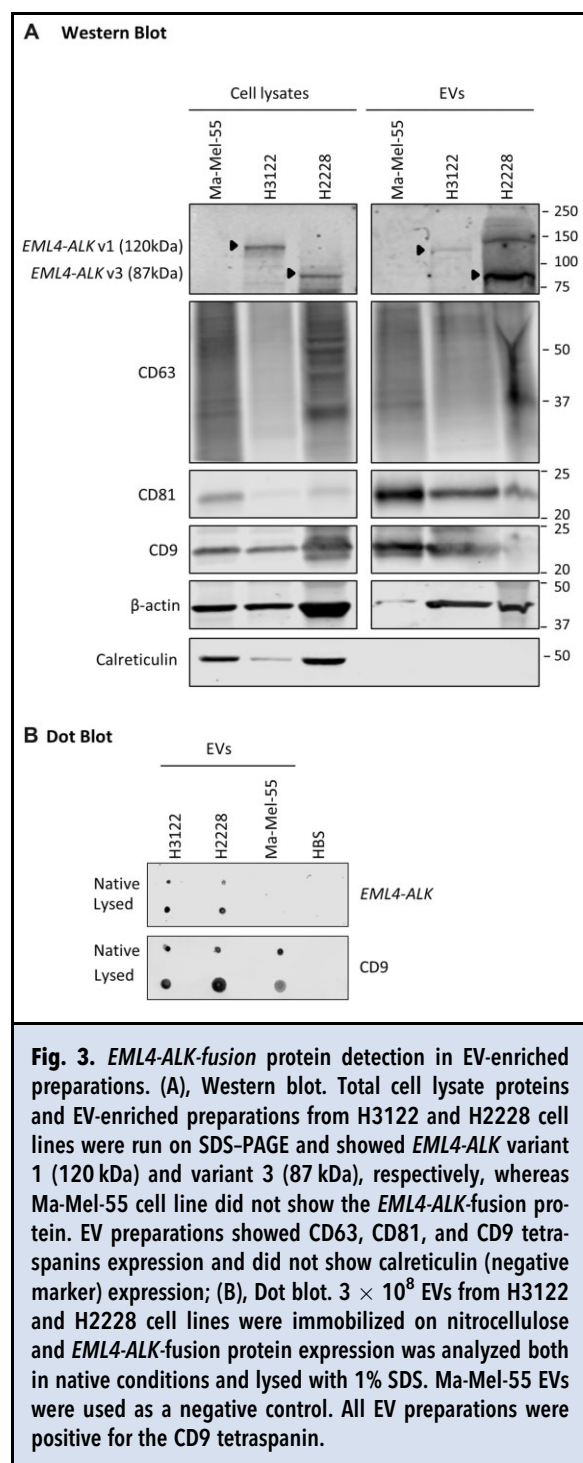
Republic)], β -actin (AC-74, Sigma-Aldrich Co.) and calreticulin (NB600-101; Novus Biologicals). Membranes were then incubated with Alexa-700-conjugated goat anti-mouse secondary antibody or Alexa-790-streptavidin secondary antibody (ThermoFisher). Proteins were visualized using the Odyssey Infrared system (LI-COR Biosciences).

EXOVIEW ANALYSIS

Complete characterization of plasma-derived EVs ($N=2$) was performed by ExoView R100 (NanoView Biosciences) using human tetraspanins kits (EV-DTETRA-C). Chips were prescanned using the provided protocol to identify any previously adhered particles during manufacturing. For incubation, chips were placed in 12-well plates, avoiding contact of the chip corners with the sides of the well. EVs were diluted at 1:100 in the provided incubation solution buffer; 50 μ L of the diluted sample was incubated overnight without agitation. Following the manufacturer's protocol, several washes were performed the following day. Then, 1 μ g/mL of fluorescently labeled antibodies provided by the kit anti-CD9 kit (CF 488A), anti-CD63 (CF 647A), and the protein of interest anti-*ALK*-(CF 594A) labeled by Alexa Fluor 594 Conjugation Kit Fast (ab269822, ABCAM) were incubated for 1 hour with gentle agitation. The chips were then washed and dried for analysis using ExoView Analyzer (Nanoview Biosciences).

RNA ISOLATION AND QUALITY ASSESSMENT

RNA from EV preparations (50 μ L each) was isolated using exoRNeasy[®] Serum/Plasma Maxi Kit (QIAGEN), following the manufacturer's instructions after EVs lysis with QIAzol reagent (QIAGEN). Samples were eluted in 14 μ L of RNase-free water. EV RNA samples were analyzed with the Agilent RNA 6000 Pico Kit using Agilent 2100 Bioanalyzer (Agilent Technologies).



RNA from supernatants obtained by ultracentrifugation of cell medium and plasma were isolated using QIAamp[®] Circulating Nucleic Acid Kit (QIAGEN), following the manufacturer's instructions.

Finally, 6.5 μ L of total RNA was reverse-transcribed into complementary DNA (cDNA) using the PrimeScript RT Reagent Kit (TaKaRa) according to the manufacturer's recommendations.

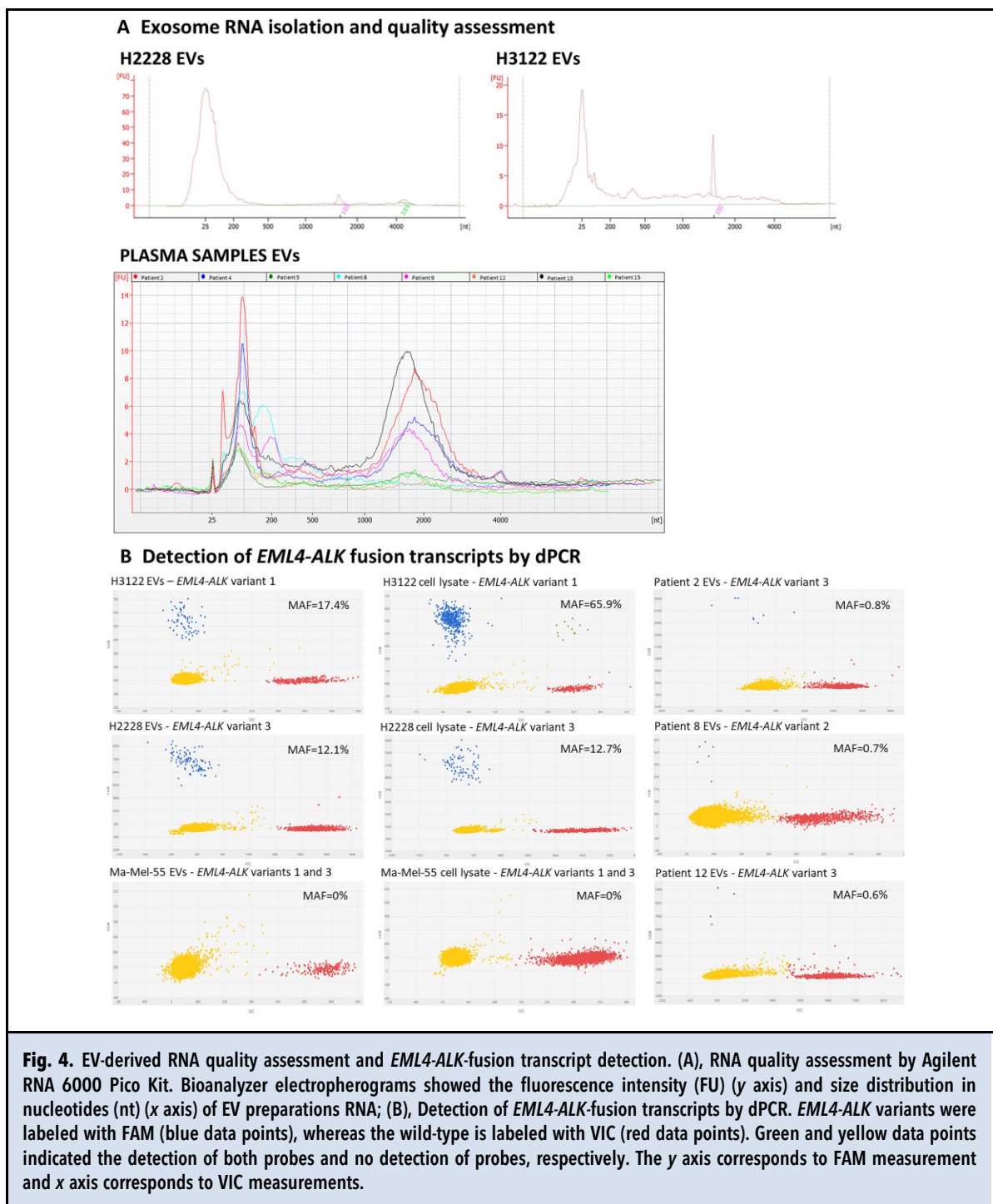
DIGITAL PCR

ALK-fusion variants were analyzed by digital PCR (dPCR) using a QuantStudio[®] 3D Digital PCR System (Applied Biosystems) as previously described (14, 15). Assays for *ALK*-fusion variants are presented in Supplemental Table S1, as endogenous gene we used the *PUM1* (Hs00472881_m1) assay. A blank (with no cDNA), a negative control [a wild-type (WT) cDNA], and a positive control (H2228 and H3122 cell lysates) were included in each dPCR run. The mutant allele frequency (MAF) was calculated as the ratio of mutant (mut) DNA molecules to the total number of molecules (sum of mutant and WT molecules). Detailed information about the sensitivity of the dPCR *EML4-ALK* TaqMan[®] assays is available in the Supplemental Methods.

Results

EML4-ALK FUSION CAN BE DETECTED IN EV PREPARATIONS FROM NSCLC CELL LINES

To determine whether *EML4-ALK* translocations are present in NSCLC EV-enriched samples, we used culture supernatants from H3122 and H2228 cell lines. The metastatic melanoma cell line Ma-Mel-55, lacking these rearrangements, was used in parallel as a negative control. EV-enriched preparations were obtained by sequential centrifugation of the conditioned medium and were fully characterized following MISEV2018 guidelines (16). According to NTA the diameter of the particles ranged from 50 to 350 nm with means of 216 nm, 229 nm, and 193 nm and modes of 155 nm, 127 nm, and 128 nm, for H3122, H2228, and Ma-Mel-55 cell lines, respectively (Fig. 1, A), consistent with the size of small-medium EVs described in the literature. Similarly, TEM analysis of the EV-enriched preparations showed 50–300 nm spherical vesicles with the typical cup-shaped morphology, described to be caused by dehydration of vesicles during sample treatment processing for TEM (Fig. 1, B). Gold immunolabeling of CD9 and CD81 showed vesicles carrying these proteins in the EV preparations from the 3 cell lines. Moreover, to assess the presence of different EV-protein markers in the same particle, such as CD63, CD81, and CD9 tetraspanins, the preparation was analyzed by bead-assisted flow cytometry. EVs were captured on beads coated with either tetraspanin or tumor-associated protein markers, such as EpCAM or MICA, and detected with CD9 and CD81 antibodies. Both lung cancer and metastatic



melanoma-derived EVs were analyzed. Binding was measured as a Relative Fluorescence Index (RFI) above 1. NSCLC cells clearly contained EpCAM and CD63 in CD9- and CD81-positive vesicles while metastatic melanoma was positive for the immune-activating ligand MICA, indicating the presence of these protein

combinations in the fraction of the EV preparations (Fig. 1, C).

Once the EV preparations were characterized using several standard techniques, the presence of *EML4-ALK*-fusion proteins was evaluated by confocal microscopy and western blot, together with transmembrane

EV-protein markers. Dual labeling of EVs with anti-*ALK* and anti-CD63 antibodies was observed, by confocal microscopy, in H3122 and H2228 EV preparations whereas Ma-Mel-55 EVs only showed CD63 expression (Fig. 2, A, Supplemental Fig. S1). In approximately 30% of EVs, we could detect both markers in the same vesicle. EV preparations were negative for the endoplasmic reticulum protein calreticulin expression (Fig. 2, A and Supplemental Fig. S1). RNA-FISH confirmed the presence of *ALK*-fusion transcripts in H3122 (variant 1) and H2228 (variant 3) derived EVs (Fig. 2, C). Likewise, we corroborated the presence of *ALK-EML4*-fusion protein in EVs by western blot analysis. As presented in Fig. 3, A *EML4-ALK* variant 1 (E13; A20) (120 kDa) and variant 3 (E6a/b; A20) (87 kDa) fusion proteins were clearly detected in H3122 and H2228 cell lysates and EV fractions, respectively, whereas no *ALK*-fusion variant was detected in either the EV fractions or in the lysates of the negative control Ma-Mel-55 cell line. CD63, CD9, and CD81 EV-protein markers, enriched in the EV fraction, were also detected in the same blot, as well as the cytosolic protein β -actin. Calreticulin, used as an EV-negative marker, was only detected in cell lysates. This result established that *EML4-ALK*-fusion protein variants are present and can be detected in EVs derived from tissue culture supernatants of NSCLC cell lines. In addition, we performed a dot blot analysis of the EVs either in their native state or after lysis with 1% SDS. As shown in Fig. 3, B, the tetraspanin CD9 was similarly detected on vesicles in their native state and in the lysed vesicles, indicating that this protein is recognized by the antibody at the vesicle surface. Regarding *EML4-ALK* protein, the positive signal was lower in the native state compared to the lysed vesicles, suggesting that the antibody was recognizing the protein predominantly inside the vesicle (Fig. 3, B). This result also supported the presence of the protein within EVs and not as a coprecipitating aggregate in the EV preparation. The low signal observed in native vesicles could be due to the disruption of a small proportion of the EV membranes on immobilization on the nitrocellulose. *EML4-ALK*-fusion proteins were not detected in Ma-Mel-55 cell lines.

EV-derived RNA from cell lines was analyzed by Agilent RNA 6000 Pico Kit using an Agilent 2100 Bioanalyzer. For both lung cancer cell lines, we mainly identified small RNAs (<200 nt) (H3122 EVs RNA area = 117.1 nt; H2228 EVs RNA area = 67.5 nt), although 18S and 28S rRNA peaks were weakly present (Fig. 4, A). Finally, as shown in Fig. 4, B, dPCR analysis detected *EML4-ALK* variant 1 and variant 3 transcripts in H3122 and H2228 cell lysates, respectively (MAF = 65.9% and MAF = 12.7%, respectively) and EV fractions (MAF = 17.4% and MAF = 12.1%, respectively), whereas the signal was negligible in the corresponding supernatant (Supplemental Fig. S4).

Additionally, for the negative control Ma-Mel-55 cell line no *ALK*-fusion transcript variant was detected either in the EV fractions or in the lysates (Fig. 4, B).

***EML4-ALK* FUSION CAN BE DETECTED IN EV PREPARATIONS FROM NSCLC PATIENT PLASMA SAMPLES**

To investigate whether *ALK* fusions were detectable in EVs isolated from clinical samples, plasma-derived EVs from NSCLC patients ($N=3$) were characterized in terms of size distribution and number of particles by NTA (Fig. 5, A), showing a profile similar to that of the NSCLC cell-derived EVs (Fig. 1). Similarly, CD63, CD81, and CD9 tetraspanins coexpression was confirmed in plasma EVs by flow cytometry ($N=3$) (Fig. 5, B). In addition, *ALK*-fusion protein was clearly detected in the plasma-derived-EVs from *ALK*-positive NSCLC patients ($N=2$), using ExoView. Indeed, CD81, CD63, and CD9 captured EV populations contained *ALK*-fusion protein, most notably in CD81-captured EVs (Fig. 5, C and D and Supplemental Fig. S2).

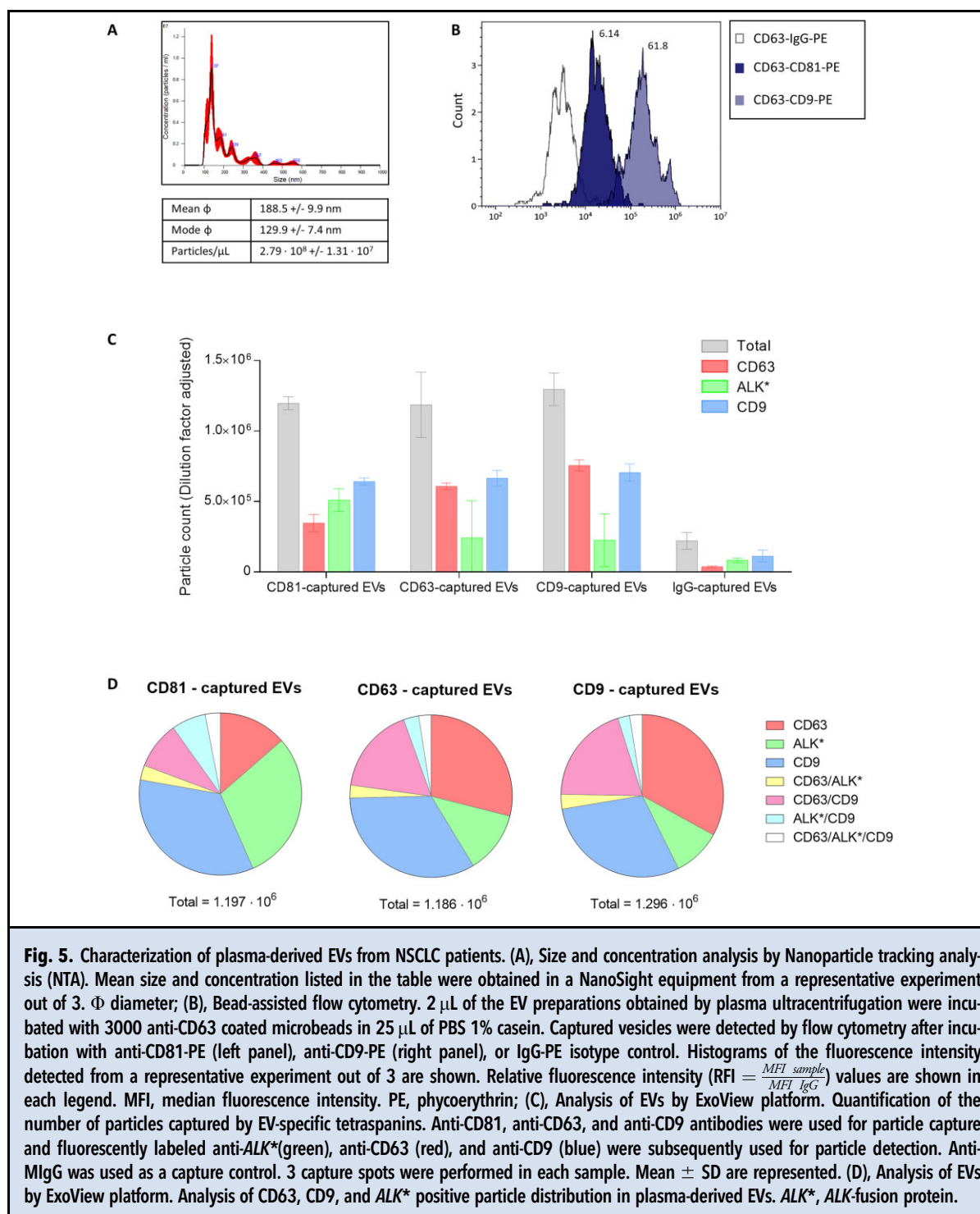
To further characterize the presence of *ALK* rearrangements in plasma-derived EVs, we evaluated the detection of the 3 most common *EML4-ALK*-fusion variants (Supplemental Table S1) at the RNA level by analyzing their corresponding cDNA by dPCR (Fig. 4 and online Supplemental Fig. S3).

To this end, EVs were isolated from the pretreatment plasma sample from 16 *ALK*-positive NSCLC patients. Clinical characteristics of the study population are presented in Supplemental Table S2. Overall, the median concentration of EV-derived RNA from NSCLC patients was 0.618 ng/ μ L. Small RNAs (<500 nt) were detected in all EV preparations using Bioanalyzer 2100. In addition, 9 patients showed a 2000–4000 nt peak (Fig. 4).

As presented in Table 1, *EML4-ALK* variant 1 (E13; A20) was detected in 2 patients (12.5%), *EML4-ALK* variant 2 (E20; A20) was detected in 1 patient (6.3%) and *EML4-ALK* variant 3 (E6a/b; A20) was detected in 5 patients (31.3%), with a detection rate of 50%. No *ALK*-fusion transcript was detected in the supernatant obtained after plasma ultracentrifugation ($N=2$) (Supplemental Fig. S4).

Discussion

Liquid biopsies are increasingly used in daily oncology practice as they provide a noninvasive way to identify biomarkers. Specifically, in NSCLC patients there is growing evidence supporting the use of liquid biopsies for Epidermal Growth Factor Receptor (*EGFR*) testing (17, 18). Nevertheless, robust methodologies for the identification of other alterations different from single nucleotide variations (SNVs), such as *EML4-ALK* fusions, are still



lacking. Currently, the challenge is to increase the sensitivity of the blood tests for the detection of complex variants such as rearrangements in *ALK*, *ROS1*, *RET*, or *NTRK*. Notably, detecting these fusions using liquid

biopsies, although challenging, could potentially expand therapeutic options in NSCLC patients.

Several studies have shown that *ALK* rearrangements can be detected within circulating tumor cells (CTCs)

Table 1. *ALK*-fusion variants detected by dPCR, in EVs derived from the plasma samples of 16 *ALK*-positive NSCLC patients.

Patient	<i>EML4-ALK</i> variant	dPCR MAF
Patient 1	-	-
Patient 2	Variant 3 (E6a/b; A20)	0.8%
Patient 3	-	-
Patient 4	Variant 3 (E6a/b; A20)	7.1%
Patient 5	Variant 3 (E6a/b; A20)	1.5%
Patient 6	-	-
Patient 7	-	-
Patient 8	Variant 2 (E20; A20)	0.7%
Patient 9	Variant 3 (E6a/b; A20)	16.7%
Patient 10	-	-
Patient 11	-	-
Patient 12	Variant 3 (E6a/b; A20)	0.6%
Patient 13	Variant 1 (E13; A20)	6.7%
Patient 14	-	-
Patient 15	Variant 1 (E13; A20)	0.3%
Patient 16	-	-

(19, 20), although there are important concerns about the feasibility of the implementation of these methodologies in the clinical setting. Likewise, there are a few reports showing that *ALK* fusions can be detected by NGS profiling of cfDNA (21, 22). In this way, McCoach et al. reported clinical benefit from *ALK* inhibitors in 3 patients who were *ALK*-positive by NGS profiling of cfDNA despite being negative *ALK* FISH (23). Nevertheless, the use of cfDNA may have some limitations as *ALK* translocations involve a large number of base pairs, and breakpoints are usually unknown. Complex variants such as large genomic rearrangements, including translocations, can be easily detected at the RNA level as fusion transcripts. However, unlike cfDNA, RNA degrades very quickly due to RNases present in the blood, constituting a major limitation. Thus, the analysis of encapsulated RNA, protected from RNases appears to be a promising approach. With this approach, encouraging results have been reported regarding the analysis of RNA isolated from tumor educated platelets (TEPs), which are thought to be able to sequester tumor-related RNA by a microvesicle dependent mechanism (24), with a 65% sensitivity and 100% specificity for the detection of *EML4-ALK* rearrangements (25).

Likewise, noninvasive biomarker testing using EVs appears to be a promising approach. Interest in EVs was re-energized when different laboratories described the presence of RNA in vesicles (26). To our knowledge, this

is the first study thoroughly demonstrating that *ALK* fusions are present and can be detected in EV preparations from *ALK*-positive NSCLC cells and plasma samples from NSCLC patients. We were able to demonstrate the presence of an *ALK*-fusion transcript in EVs isolated from 8 plasma samples from patients who were previously diagnosed as having NSCLC harboring an *ALK*-fusion. Currently, there is intense research aimed to improve the technology for the characterization and phenotyping of EVs and validation of EVs for biomarker identification (27, 28). Size-exclusion chromatography (SEC) has been shown to perform well in separating EVs from clinical samples (29) and an automatic exosome isolation system based on SEC has been developed (qEV Automatic Fraction Collector). Likewise, high sensitivity methods for EV detection based on immune-capture have been described (13). Similarly, an automated, point-of-care device capable of isolating exosomes directly from whole blood has been developed by integrating acoustics and microfluidics (30), suggesting that robust high-throughput EV isolation methods will be available in the near future. In this regard, our results set the basis for noninvasive *ALK*-fusion transcript detection using EV preparations. Remarkably, unraveling the tetraspanin and *ALK*-fusion protein colocalization patterns will be vital for the development of EV-based diagnostic tests. As an exploratory analysis, our data, show that CD81-captured EVs are enriched in *ALK*-fusion protein. These findings should be confirmed in an appropriately sized cohort.

Different RNA populations have been identified in EVs (31–34). According to our data, the RNAs from EVs were mostly small RNAs (<200 nt), although 18S and 28S rRNA peaks were also detected in cell line samples. In some clinical samples, the electrophoretic pattern was compatible with the presence of long noncoding RNAs. Nevertheless, RNA obtained from EVs can be highly affected by the extraction method and studies on EV RNAs characterization remains lacking.

In summary, we have shown here that *ALK* fusions are present in EVs from NSCLC cells and patients. Although further improvements in EV isolation methods are needed, our results indicate that *ALK*-fusion testing through liquid biopsy is feasible. These results set the stage for high-throughput methodologies for fusion transcript detection on liquid biopsies.

ETHICS APPROVAL AND CONSENT TO PARTICIPATE

The study protocol was approved by the Hospital Puerta de Hierro Ethics Committee (internal code 79-18), and was conducted in accordance with the precepts of the Code of Ethics of The World Medical Association (Declaration of Helsinki). All patients provided their appropriate written informed consent to participate in the study prior to enrollment.

CONSENT FOR PUBLICATION

We have obtained consent to publish this paper from all of the study participants.

Supplemental Material

Supplemental material is available at *Clinical Chemistry* online.

Nonstandard Abbreviations: NSCLC, nonsmall cell lung cancer; EVs, extracellular vesicles; TEM, transmission electron microscopy; NTA, nanoparticle tracking analysis; dPCR, digital PCR; ALK, anaplastic lymphoma kinase; ctDNA, circulating tumor DNA; cfRNA, circulating free RNA; FISH, fluorescence in situ hybridization; cDNA, complementary DNA; WT, wild-type; MAF, mutant allele frequency; mut, mutant; RFI, relative fluorescence intensity; EGFR, epidermal growth factor receptor; SNVs, single nucleotide variations; CTCs, circulating tumor cells; TEPs, tumor educated platelets; SEC, size-exclusion chromatography; MFI, mean fluorescence intensity; PE, phycoerythrin; FU, fluorescence intensity

Human Genes: *ALK*, ALK receptor tyrosine kinase; *EGFR*, epidermal growth factor receptor; *EML4*, EML4 like 4; *NTRK*, neurotrophic receptor tyrosine kinase 1; *PUM1*, pumilio RNA binding family member 1; *RET*, ret proto-oncogene; *ROS1*, ROS proto-oncogene 1, receptor tyrosine kinase.

Acknowledgments: H. Peinado (CNIO) for the use of NanoSight; V. Horejsi (Inst. of Molecular Genetics Academy of Sciences of the Czech Republic, Prague) for tetraspanin antibodies. M. A. Molina for H3122 and H2228 cell lines; Annette Paschen (University Hospital Essen, Germany) for Ma-Mel-55 cell line.

Author Contributions: All authors confirmed they have contributed to the intellectual content of this paper and have met the following 4 requirements (a) significant contributions to the conception and design, acquisition of data, or analysis and interpretation of data; (b) drafting or revising the article for intellectual content; (c) final approval of the published article; and (d) agreement to be accountable for all aspects of the article thus ensuring that questions related to the accuracy or integrity of any part of the article are appropriately investigated and resolved.

Conception and design, V. González-Rumayor, M. Valés-Gómez, M. Provencio, and A. Romero. Development of methodology, E. Sánchez-Herrero, C. Campos-Silva, Y. Cáceres-Martell, S. Sanz-Moreno, A. Rodríguez-Festa, D. Ares Trotta, C. Patiño, M.J. Coronado, A. Beneitez, R. Jara, N. Lago-Baameiro, T. Camino, L. Robado de Lope, and A. Cruz-Bermúdez. Acquisition of data, E. Sánchez-Herrero, P. Martín-Acosta, M. Provencio, and A. Romero. Analysis and interpretation of data, E. Sánchez-Herrero, C. Campos-Silva, Y. Cáceres-Martell, R. Serna-Blasco, M. Valés-Gómez, and A.

Romero. Writing, review, and/or revision of the manuscript, E. Sánchez-Herrero, C. Campos-Silva, Y. Cáceres-Martell, L. Robado de Lope, V. González-Rumayor, M. Valés-Gómez, M. Provencio, and A. Romero. Administrative, technical, or material support, P. Martín-Acosta, C. Patiño, M.J. Coronado, A. Beneitez, R. Jara, and M. Pardo. Study supervision, V. González-Rumayor, M. Valés-Gómez, M. Provencio, and A. Romero. Approved manuscript, All authors.

Authors' Disclosures or Potential Conflicts of Interest: Upon manuscript submission, all authors completed the author disclosure form. Disclosures and/or potential conflicts of interest:

Employment or Leadership: R. Jara is CEO of Immunostep, S.L.; A. Beneitez is employee of Immunostep, S.L.

Consultant or Advisory Role: A. Romero, Takeda

and M. Provencio, BristolMyers Squibb, Takeda, Roche, AstraZeneca, Merck Sharpe & Dohme.

Stock Ownership: None declared.

Honoraria: None declared.

Research Funding: This study has been funded by Instituto de Salud Carlos III through the project "PI17/01977" (co-funded by European Regional Development Fund/European Social Fund "A way to make Europe"/"Investing in your future"). The work presented in this paper also received funding from the European Union's Horizon 2020 research and innovation program under grant agreement No 875160. E. Sánchez-Herrero was funded by the Consejería de Ciencia, Universidades e Innovación of the Comunidad de Madrid (Doctorados Industriales of the Comunidad de Madrid IND2019/BMD-17258). R. Serna-Blasco was funded by the Consejería de Educación, Juventud y Deporte of the Comunidad de Madrid and by the Fondo Social Europeo (Programa Operativo de Empleo Juvenil, and Iniciativa de Empleo Juvenil, PEJD-2018-PRE/BMD-8640). M. Valés-Gómez was funded by Spanish Ministry of Science and Innovation (MCIU/AEI/FEDER, EU) grant RTI2018-093569-B-I00 and Madrid Regional Government under grant "IMMUNOTHERCAN" (S2017/BMD-3733-2). This work was supported by GEIVEX, Network of Excellence in the Research and Innovation on Exosomes REDIEX, SAF2015-71231-REDT, Network of Excellence in Translational NeTwork for the CLInical application of Extracellular VesicleS (TeNTaCLES) (RED2018-102411-T). M. Provencio, grants from BristolMyers Squibb, Roche, and AstraZeneca.

Expert Testimony: None declared.

Patents: M. Valés-Gómez, Y. Cáceres-Martell, and C. Campos-Silva, EP1641.1562 Method for the detection and/or quantification of extracellular vesicles in fluid biological samples.

Other Remuneration: A. Romero reports personal fees from Takeda, outside the submitted work. M. Provencio reports personal fees, and travel expenses from BristolMyers Squibb, Roche, and AstraZeneca; and personal fees from Merck Sharpe & Dohme and Takeda, outside the submitted work. M. Valés-Gómez, Licence of ExostepTM to Immunostep S.L.

Role of Sponsor: The funding organizations played no role in the design of study, choice of enrolled patients, review and interpretation of data, preparation of manuscript, or final approval of manuscript.

REFERENCES

- Gainor JF, Varghese AM, Ou SHI, Kabraji S, Awad MM, Katayama R, et al. ALK rearrangements are mutually exclusive with mutations in EGFR or KRAS in analysis of 1,683 patients with non-small cell lung cancer. *Clin Cancer Res* 2013;19:4273-81.
- Koivunen JP, Mermel C, Zejnullahu K, Murphy C, Lifshits E, Holmes AJ, et al. EML4-ALK fusion gene and efficacy of an ALK kinase inhibitor in lung cancer. *Clin Cancer Res* 2008;14:4275-83.
- Zhang X, Zhang S, Yang X, Yang J, Zhou Q, Yin L, et al. Fusion of EML4 and ALK is associated with development of lung adenocarcinomas lacking EGFR and KRAS mutations and is correlated with ALK expression. *Mol Cancer* 2010;9:188.
- Childress MA, Himmelberg SM, Chen H, Deng W, Davies MA, Lovly CA. Fusion partners impact response to ALK inhibition differential effects on sensitivity, cellular phenotypes, and biochemical properties. *Mol Cancer Res* 2018;16:1724-36.
- Shaw AT, Kim DW, Nakagawa K, Seto T, Crinó L, Ahn MJ, et al. Crizotinib versus chemotherapy in advanced ALK-positive lung cancer. *N Engl J Med* 2013;368:2385-94.
- Gadgeel SM, Gandhi L, Riely GJ, Chiappori AA, West HL, Azada MC, et al. Safety and activity of alectinib against systemic disease and brain metastases in patients with crizotinib-resistant ALK-rearranged nonsmall-cell lung

- cancer (AF-002JG). Results from the dose-finding portion of a phase 1/2 study. *Lancet Oncol* 2014;15:1119-28.
7. Duruisseaux M, Besse B, Cadranet J, Pérol M, Mennecier B, Bigay-Game L, et al. Overall survival with crizotinib and next-generation ALK inhibitors in ALK-positive non-small-cell lung cancer (IFCT-1302 CLINALK): a French nationwide cohort retrospective study. *Oncotarget* 2017;8:21903-17.
 8. NCCN Guidelines. For Patients[®] non-small cell lung cancer metastatic. <http://NCCN.org/patients> (Accessed 22 Jul 2021).
 9. Supplee JG, Milan MSD, Lim LP, Potts KT, Sholl LM, Oxnard GR, et al. Sensitivity of next-generation sequencing assays detecting oncogenic fusions in plasma cell-free DNA. *Lung Cancer* 2019;134:96-9.
 10. Arroyo JD, Chevillet JR, Kroh EM, Ruf IK, Pritchard CC, Gibson DF, et al. Argonaute2 complexes carry a population of circulating microRNAs independent of vesicles in human plasma. *Proc Natl Acad Sci USA* 2011;108:5003-8.
 11. Deatherage BL, Cookson BT. Membrane vesicle release in bacteria, eukaryotes, and archaea: a conserved yet underappreciated aspect of microbial life. *Infect Immun* 2012;80:1948-57.
 12. López-Cobo S, Pieper N, Campos-Silva C, García-Cuesta EM, Reyburn HT, Paschen A, Valés-Gómez M. Impaired NK cell recognition of vemurafenib-treated melanoma cells is overcome by simultaneous application of histone deacetylase inhibitors. *Oncoimmunology* 2018;7:e1392426.
 13. Campos-Silva C, Cáceres-Martell Y, López-Cobo S, Rodríguez MJ, Jara R, Yáñez-Mó M, Valés-Gómez M. An immunocapture-based assay for detecting multiple antigens in melanoma-derived extracellular vesicles. *Methods Mol Biol* 2021;2265:323-44.
 14. Romero A, Serna-Blasco R, Alfaro C, Sánchez-Herrero E, Barquín M, Turpin MC, et al. ctDNA analysis reveals different molecular patterns upon disease progression in patients treated with osimertinib. *Transl Lung Cancer Res* 2020;9:532-40.
 15. Sánchez-Herrero E, Serna-Blasco R, Ivanchuk V, García-Campelo R, Dómine Gómez M, Sánchez JM, et al. NGS-based liquid biopsy profiling identifies mechanisms of resistance to ALK inhibitors: a step toward personalized NSCLC treatment. *Mol Oncol* 2021;15:2363-76.
 16. Théry C, Witwer KW, Aikawa E, Alcaraz MJ, Anderson JD, Andriantsitohaina R, et al. Minimal information for studies of extracellular vesicles 2018 (MISEV2018): a position statement of the International Society for Extracellular Vesicles and update of the MISEV2014 guidelines. *J Extracell Vesicles* 2018;7:1535750.
 17. Romero A, Jantus-Lewintre E, García-Peláez B, Royuela A, Insa A, Cruz P, et al. Comprehensive cross-platform comparison of methods for non-invasive EGFR mutation testing: results of the RING observational trial. *Mol Oncol* 2021;15:43-56.
 18. Ettinger DS, Wood DE, Aggarwal C, Aisner DL, Akerley W, Bauman JR, et al.; OCN. Non-small cell lung cancer, version 1.2020: featured updates to the NCCN guidelines. *J Natl Compr Cancer Netw* 2019;17:1464-72.
 19. Aieta M, Facchinetti A, De Faveri S, Manicone M, Tartarone A, Possidente L, et al. Monitoring and characterization of circulating tumor cells (CTCs) in a patient with EML4-ALK-positive non-small cell lung cancer (NSCLC). *Clin Lung Cancer* 2016;17:e173-77.
 20. Faugeroux V, Pailler E, Auger N, Taylor M, Farace F. Clinical utility of circulating tumor cells in ALK-positive non-small-cell lung cancer. *Front Oncol* 2014;4:281.
 21. Odegaard JI, Vincent JJ, Mortimer S, Vowles JV, Ulrich BC, Banks KC, et al. Validation of a plasma-based comprehensive cancer genotyping assay utilizing orthogonal tissue- and plasma-based methodologies. *Clin Cancer Res* 2018;24:3539-49.
 22. Pawelczak CP, Sacher AG, Raymond CK, Alden RS, O'Connell A, Mach SL, et al. Bias-corrected targeted next-generation sequencing for rapid, multiplexed detection of actionable alterations in cell-free DNA from advanced lung cancer patients. *Clin Cancer Res* 2016;22:915-22.
 23. McCoach CE, Blakely CM, Banks KC, Levy B, Chue BM, Raymond VM, et al. Clinical utility of cell-free DNA for the detection of ALK fusions and genomic mechanisms of ALK inhibitor resistance in non-small cell lung cancer. *Clin Cancer Res* 2018;24:2758-70.
 24. Nilsson RJA, Balaj L, Hulleman E, Van Rijn S, Pegtel DM, Walraven M, et al. Blood platelets contain tumor-derived RNA biomarkers. *Blood* 2011;118:3680-3.
 25. Nilsson RJA, Karachaliou N, Berenguer J, Gimenez-Capitan A, Schellen P, Teixido C, et al. Rearranged EML4-ALK fusion transcripts sequester in circulating blood platelets and enable blood-based crizotinib response monitoring in non-small-cell lung cancer. *Oncotarget* 2016;7:1066-75.
 26. Valadi H, Ekström K, Bossios A, Sjöstrand M, Lee JJ, Lötvall JO. Exosome-mediated transfer of mRNAs and microRNAs is a novel mechanism of genetic exchange between cells. *Nat Cell Biol* 2007;9:654-9.
 27. Liang Y, Lehrich BM, Zheng S, Lu M. Emerging methods in biomarker identification for extracellular vesicle-based liquid biopsy. *J Extracell Vesicles* 2021;10:e12090.
 28. Bordanaba-Florit G, Royo F, Kruglik SG, Falcón-Pérez JM. Using single-vesicle technologies to unravel the heterogeneity of extracellular vesicles. *Nat Protoc* 2021;16:3163-85.
 29. Böing AN, van der Pol E, Grootemaat AE, Coumans FAW, Sturk A, Nieuwland R. Single-step isolation of extracellular vesicles by size-exclusion chromatography. *J Extracell Vesicles* 2014;3:23430.
 30. Fais S, O'Driscoll L, Borrás FE, Buzas E, Camussi G, Cappello F, et al. Evidence-based clinical use of nanoscale extracellular vesicles in nanomedicine. *ACS Nano* 2016;10:3886-99.
 31. Kim KM, Abdelmohsen K, Mustapic M, Kapogiannis D, Gorospe M. RNA in extracellular vesicles. *Wiley Interdiscip Res RNA* 2017;8:e1413.
 32. Nolte-t Hoen ENM, Buermans HPJ, Waasdorp M, Stoorvogel W, Wauben MHM, 't Hoen PAC. Deep sequencing of RNA from immune cell-derived vesicles uncovers the selective incorporation of small noncoding RNA biotypes with potential regulatory functions. *Nucleic Acids Res* 2012;40:9272-85.
 33. Crescitelli R, Lässer C, Szabó TG, Kittel A, Eldh M, Dianzani I. Distinct RNA profiles in subpopulations of extracellular vesicles: apoptotic bodies, microvesicles and exosomes. *J Extracell Vesicles* 2013;2:20677.
 34. Zhang S, Du L, Wang L, Jiang X, Zhan Y, Li J, et al. Evaluation of serum exosomal lncRNA-based biomarker panel for diagnosis and recurrence prediction of bladder cancer. *J Cell Mol Med* 2019;23:1396-405.